water

MDPI

Article

A Route Search System to Avoid the Danger to Life in Dynamic Inundation

Kohei Ogawa [1], Takuya Inoue [1,*], Yuki Hiramatsu [2] and Jagriti Mishra [3]

[1] Graduate School of Advanced Science and Engineering, Hiroshima University, Higashihiroshima 739-8551, Japan
[2] Civil Engineering Research Institute for Cold Region, Sapporo 062-8602, Japan
[3] School of Environmental Sciences, Jawaharlal Nehru University, New Delhi 110067, India
* Correspondence: inouetakuya@hiroshima-u.ac.jp; Tel.: +81-82-424-7817

Abstract: In recent years, the frequency of torrential rains has increased due to abnormal weather conditions. Torrential rains have caused extensive flooding damage in many areas. As delays in evacuation can pose a threat to life, a quick search for safe evacuation routes has become more important than ever before. In this study, we constructed a new system for searching evacuation routes that incorporates a function that varies the weight of each road in the route search depending on the distance from the flooded area D and the distance that the flood area extends in 10 min D' (i.e., the flood's inundation speed). We conducted multiple hypothetical flood simulations with different locations of levee breaches and shelters in the study site (Obihiro City, Japan). Then, we compared the results with the conventional system that does not include the proposed function. The results showed that the system proposed in this study increased the number of successful evacuees by up to 2.16 times compared to the conventional system. In our system, the weight function is set to the C_d power of D/D'; increasing the model parameter C_d selects a route that detours more of the flooded area. The model parameter C_d that maximizes the number of successful evacuees is roughly constant, regardless of the locations of the levee breaches or shelters in the study site.

Keywords: flood; evacuation; route search; levee breech; shelter

Citation: Ogawa, K.; Inoue, T.; Hiramatsu, Y.; Mishra, J. A Route Search System to Avoid the Danger to Life in Dynamic Inundation. *Water* **2023**, *15*, 1417. https://doi.org/10.3390/w15071417

Academic Editors: Dimitrios A. Emmanouloudis, Elissavet G. Feloni, Fotis Maris and Panagiotis Nastos

Received: 14 February 2023
Revised: 25 March 2023
Accepted: 3 April 2023
Published: 5 April 2023

1. Introduction

Global warming, environmental destruction, and urbanization have exposed many people to the threat of natural disasters. Of the 432 recorded catastrophic events in 2021, floods are the most dominant factor, accounting for about 50% of the total disasters. Flood disasters have been particularly severe in Asia; during its monsoon season, India experienced large floods that claimed 1282 lives, and in July, the Henan floods in China killed 352 people and affected 14.5 million people [1]. The flood damage statistical survey results of the Ministry of Land, Infrastructure, Transport, and Tourism of Japan show that average annual flood damage has been increasing in recent years in Japan: 212 billion yen from 2006–2010; 433 billion yen from 2011–2015; and 1111 billion yen from 2016–2020 [2].

Frequent and severe floods have increased the importance of information on evacuation routes, shelters, and warnings. Previous studies on evacuation routes have typically focused on understanding the behavioral characteristics of evacuees and the dynamics of traffic flow, e.g., [3–5], to systematically identify optimal routes and shelter locations, e.g., [6–8], and clarify the effects of flow velocity and depth on stability failures of people, such as sliding in floodwater, e.g., [9–11]. For example, Robinson and Khattak (2010) proposed a dynamic traffic simulation with a decision model to assess the impact of driver decisions during evacuation [5]. Chelariu et al. (2022) developed a tool that uses spatial analysis techniques to analyze the time required to evacuate a certain area to achieve an organized and safe evacuation of residents [7]. Musolino et al. (2020) showed that walkability criteria based on flood characteristics and the corresponding stability of the human

body are suitable for identifying optimal evacuation routes [9]. Although these studies have improved the quality of evacuation planning, a major problem with evacuation is that many people are not motivated to evacuate by official warnings alone [12,13].

In recent years, tools with real-time flood mapping coupled with route searching are expected to motivate people to evacuate. The technology of flood mapping using numerical analysis [14], IoT [15], and satellite imagery [16] is advancing day by day, and in Tokyo, Japan, the real-time flood mapping system "S-uiPS" has been open to the public since September 2022 [17,18]. The realization of real-time flood mapping has driven the development of real-time evacuation routing systems [19–22]. Inoue et al. (2018) developed a real-time evacuation routing system based on real-time 2D flood analysis at 25m resolution and route search with a set level of walking difficulty on flooded roads [19]. Lee et al. (2020) proposed an evacuation routing system considering temporal and spatial evacuation for walking hazards with an artificial neural network-based flood mapping [20].

Advances in real-time evacuation-route retrieval present us with new challenges. That is, a suggested evacuation path by retrieval may become unsafe during travel evacuation owing to an evacuee's walking speed and the speed at which floodwater spreads, resulting in evacuees being caught in floodwaters. To avoid this situation, it is proposed to evacuate while changing the evacuation route by searching at any time while moving. However, it is difficult for evacuees to keep searching while evacuating, and the continuous change of evacuation routes may confuse evacuees. Another method is to search for evacuation routes using future forecasts of the inundated area. While this method appears to be effective, it is difficult to provide highly accurate evacuation routes, given the uncertainty of current weather forecasts.

In this study, we propose a new evacuation route search system that considers the speed of expansion of the flooded area to avoid the risk of being caught in flooding during an evacuation. Specifically, the priority of routes is weighted using the ratio between the distance from the flooded area to each road and the flood's inundation speed, simply estimated from the known current and past flood mapping. Note that since this study focuses on the development of a routing system, we didn't perform real-time flood mapping. Instead, we used the results of pre-computed 2D flood simulation using iRIC software [23–25] as real-time data.

2. Methods

2.1. Evacuation Route Search System

In the model proposed by Inoue et al. (2018) (hereinafter referred to as the "conventional model"), data on the flood area is read and converted into polygons in real time [19]. Next, the polygons of the flood area and each road are judged to be in contact. If there is contact, the road is deemed impassable, and the road data is removed. Then, the system searches for the shortest route to the shelter and presents a route that avoids the inundated area at the time of the route search. Although the flood area at the time of route retrieval is considered in the conventional model, changes in the flood area during travel are not considered.

The Dijkstra method, an algorithm for finding the shortest path, is used for route retrieval in the conventional model. The Dijkstra method generally inputs the distance of each road link (a road connecting two nodes) as a cost and calculates the route with the lowest cost (i.e., the shortest route). However, this method may select unsafe road links that are very close to flooded areas. Therefore, we propose a weight function that depends on D (the distance between the road link and the current flooded area) and D' (the distance between the current flooded area and the flooded area 10 min ago), as shown in Figure 1, and use this function to calculate a virtual road distance (virtual cost). We input the virtual cost into the Dijkstra method, and thus, the roads closer to the flooded area are less likely to

be selected as the shortest route. Based on the above idea, we propose Equation (1), which is a weight function, and Equation (2), which calculates the virtual cost.

$$f_d = \begin{cases} (0.01 \cdot D/D')^{Cd} & when\ D/D' \leq 100 \\ 1 & when\ D/D' > 100 \end{cases} \quad (1)$$

$$L' = \frac{L}{f_d} \quad (2)$$

where f_d is a weight function, depending on the distance to the flooded area, D is a distance between the road and the current flooded area, D' is a distance between the current flooded area and the flooded area of the previous time step, L' is a virtual distance of each road, and L is an actual distance of each road.

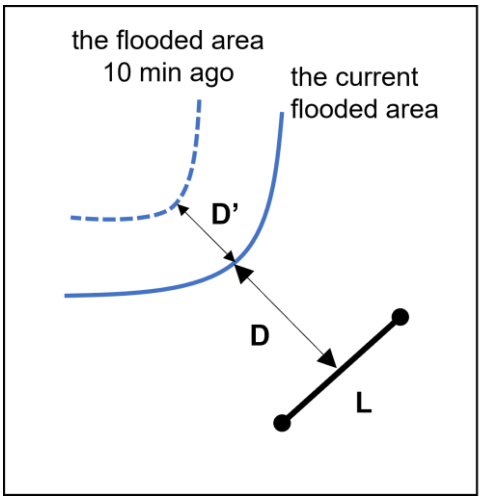

Figure 1. Schematic diagram of the weight function depending on the distance to the flooded area.

f_d takes values between 0 and 1. If the distance D between the flooded area and the road is greater than 100 times the distance D' that the flooded area spreads in 10 min (output time interval for flood simulation), it is considered safe enough, and the weight is set to 1. This means that a road link more than 100 times farther than D' will be inundated 100×10 min later. Since the total evacuation time would be 1 to 2 h at most, there is little need to consider the weight function for road links that are more than 100 times farther than D'.

Next, as shown in Equation (2), we divide the actual distance L by the f_d to obtain the virtual distance L'. By substituting L' into the Dijkstra method, a safer evacuation route that avoids roads in the vicinity of the flooded area is automatically calculated.

2.2. Evaluation Method of the System

To confirm the effectiveness of the proposed function, we evaluate the number of people who reach the shelter without being caught in the flooding (hereinafter referred to as "the number of successful evacuees"). The study site is a northern urban district in the part of Obihiro City, Hokkaido, Japan (Figure 1). Since Obihiro City is located on the alluvial fan of the Tokachi River, which flows from west to east, the elevation of the study site basically decreases from west to east. However, a terrace created by the Tokachi River is located to the south of the study site, so the elevation on the south side is slightly higher. This area is surrounded by the Tokachi River to the north and by tributaries of the Tokachi River to the south and west. Therefore, there is a high risk of flooding, and the hazard map of Obihiro City indicates that the majority of the target area is within the expected flood area.

Evacuees are placed on all 420 nodes of the road network, as shown in Figure 2. We created the road network data from Google Maps by reading the coordinates of the nodes in the study area. Note that we extracted mainly major roads that are likely to be used during an evacuation, excluding community roads. Red points represent evacuees, and purple points represent shelters. Although evacuees depart from all nodes to the shelters, the number of evacuees depends on the location of the node, such as residential areas or factory areas. Figure 3 shows the number of evacuees for each node calculated from the population distribution of Obihiro City (see Table 1). The west side has a smaller population, and the east side has a larger population. We use data on the population distribution per grid cell. The population per node is obtained by dividing the population of one cell by the number of nodes in the cell. In case a cell does not contain any nodes, the population within the cell is distributed to the four surrounding cells.

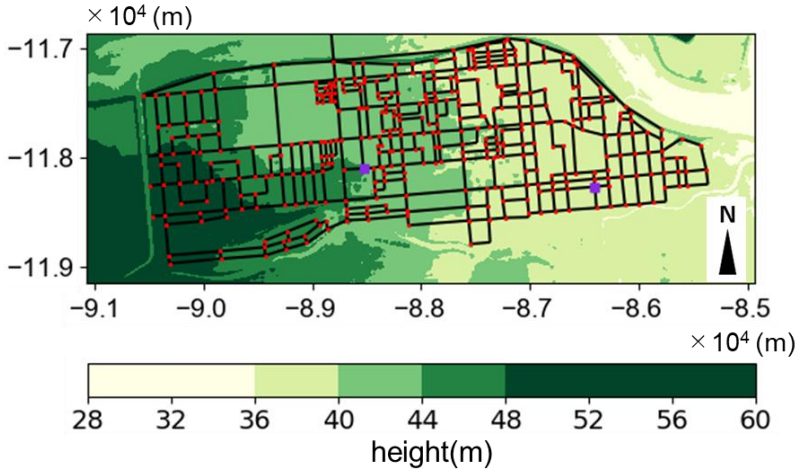

Figure 2. Load map and elevation contour map of the study site in Obihiro City, Hokkaido, Japan. Red points show the departure points of evacuees. Purple points show the two destination points (i.e., flood shelters). The x- and y-axes indicate the axis in the Japan Plane Rectangular Coordinate System XII.

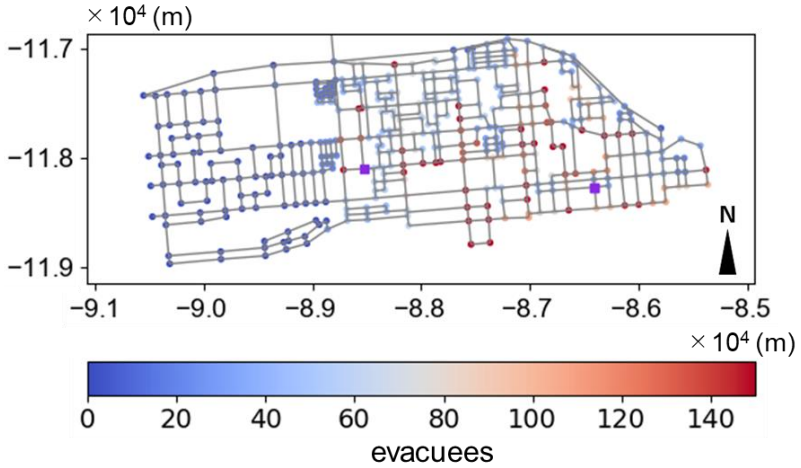

Figure 3. The population distribution of the evacuee departure points. Purple points show the two destination points (i.e., flood shelters). The x- and y-axes indicate the axis in the Japan Plane Rectangular Coordinate System XII.

Table 1. Details of the data and the software used in this study.

Data and Software	Data Sources and Links
iRIC Nays2D Flood	https://i-ric.org/en/solvers/nays2dflood/ (accessed on 17 March 2023)
Population density	https://www.e-stat.go.jp/gis (in Japanese) (accessed on 17 March 2023)
Digital Elevation Model (DEM)	https://fgd.gsi.go.jp/download/menu.php (in Japanese) (accessed on 17 March 2023) EPSG:2454: JGD2000/Japan Plane Rectangular CS XII Resolution: About 3.5 (m)

To determine if a road is impassable, data on the flooded area is needed. In the future, we plan to use the results of real-time flood analysis, but since the main focus of this study is to develop a route search system, we use our pre-calculated results instead of real-time results. We calculated the flooded area every 10 min using iRIC Nays2D flood (Nelson et al., 2016), which is free and available to all (see Table 1). The conditions used for the flood analysis are as follows. The topographic data is the Digital Elevation Model (DEM) published by the Geospatial Information Authority of Japan (GSI) (see Table 1). The grid resolution is 24 m $\times$ 30 m. Manning's roughness coefficient, which represents the resistance of the bed surface, varies with land use, but is assumed here to be a constant 0.03 for simplicity. In this study, we set up two flood patterns with different levee breach locations. The first is a fast-spreading flood, in which the river breaks its banks in the upper reaches and discharges toward areas with low elevation; the second is a slow-spreading flood, in which the river breaks its banks in the lower reaches and inundates areas with low elevation (Figure 4). In both patterns, the flow discharge from the levee breach point is a constant 500 m^3/s.

Evacuees depart from all nodes to the shelter every 10 min, e.g., 0 min, 10 min, and 20 min after the breach of the levee. Hereafter, we refer to the above departure time as "the evacuation start time". The number of evacuees at each evacuation start time is the same. The system automatically determines for each evacuee whether they are caught in the flood while walking or not. The criteria for determining whether an evacuee has been caught by the flooded area are as follows: (a) If all routes to the shelter cannot be searched because they are flooded (including the case where the starting node is flooded), the evacuee is determined to have been caught in the flooded area, i.e., an evacuation failure; (b) Contact judgment is made every 10 min between the road on which an evacuee is walking and the flooded area at that time. An evacuation is considered successful if the evacuee does not come in contact with the flooded area even once before arriving at the shelter, and an evacuation is considered unsuccessful if the evacuee comes in contact with the flooded area even once. Figure 5 shows an example of contact judgment. The dark blue area represents the flooded area at the evacuation start time, and the light blue area represents the flooded area that expands during evacuation. Our system determines whether the light blue area is contacting the road an evacuee moves on. In Figure 5b, the evacuation fails because the light blue area is in contact with the evacuation route, and in Figure 5a, the evacuation succeeds because the light blue area is not in contact with the evacuation route.

Finally, a population distribution weight for each node is applied, and the number of successful evacuees is counted. The number of successful evacuees is compared between Model I, which does not consider a weight function (i.e., the conventional model), and Model II, proposed in this study, which considers a weight function. The two models are evaluated under three conditions: Case (1) flood pattern 1 and shelter location 1; Case (2) flood pattern 2 and shelter location 2; Case (3) flood pattern 1 and shelter location 2.

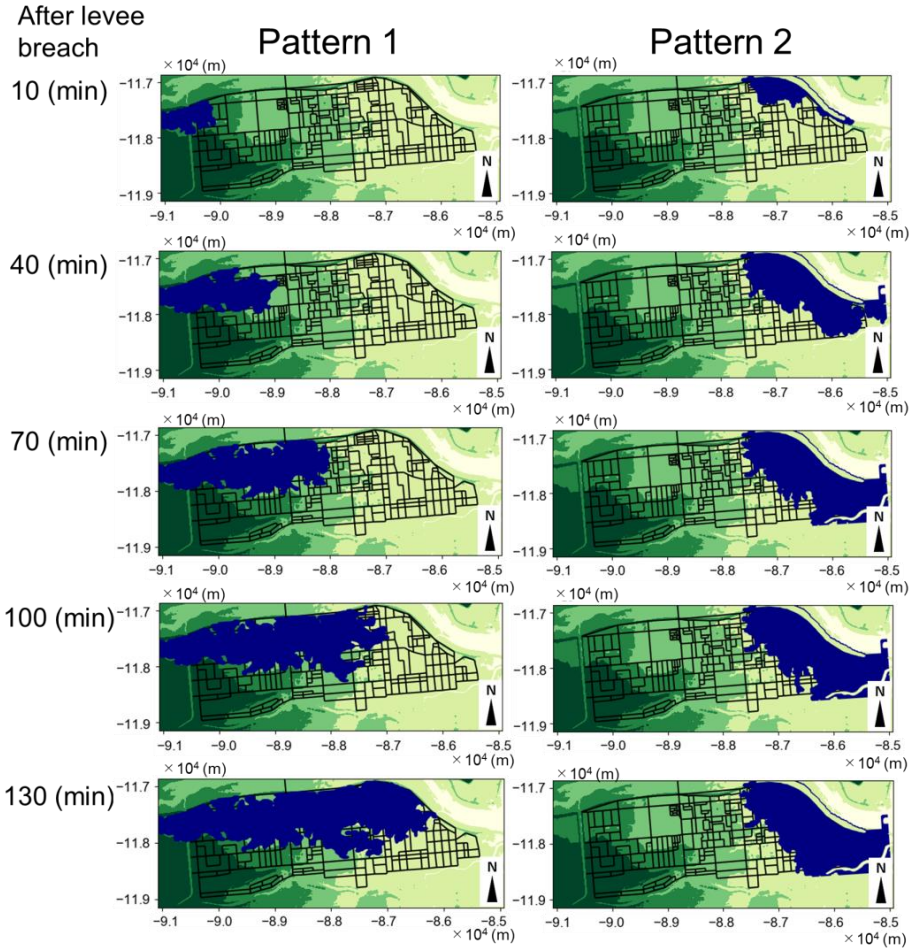

Figure 4. The results of flood simulations. Pattern 1 is the result of a levee breach upstream of the study site. Pattern 2 is the result of a levee breach downstream of the study site. Blue indicates the flooded area.

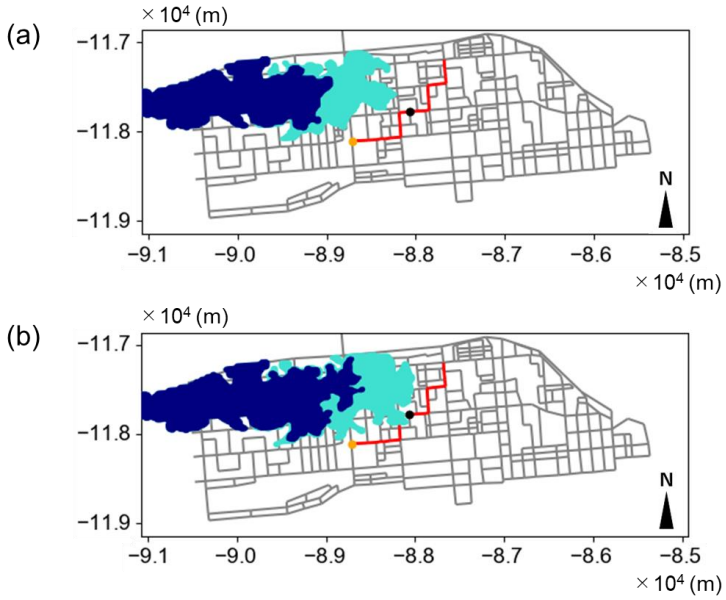

Figure 5. Criteria for disaster assessment: (**a**) evacuation success; (**b**) evacuation failure. Blue shows the inundation area at the start of the evacuation; light blue shows the inundation area at the time the evacuees walked to the point of the black dot. The red line marks the evacuation route. The x- and y-axes indicate the axis in the Japan Plane Rectangular Coordinate System XII.

3. Results and Discussion

An example of the evacuation route using Model I and Model II is shown in Figure 6. The yellow line shows the evacuation route for Model I, and the red line for Model II. The dark blue area indicates the flooded area at the time of the route search (at the start of evacuation). It shows that Model II selects a route with more distance between the flooded area and the route than Model I.

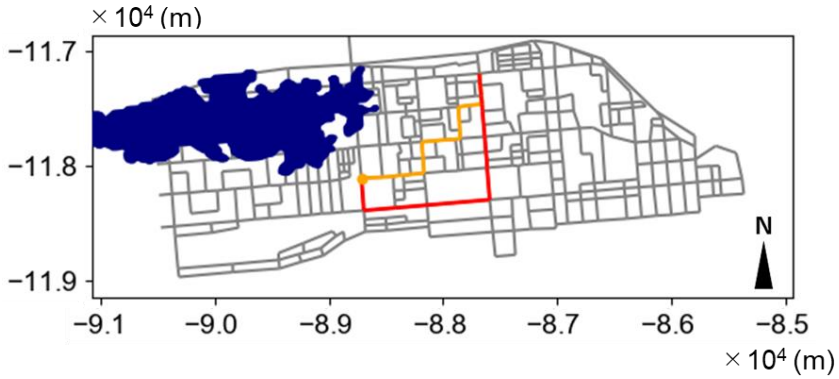

Figure 6. Example of evacuation route by Model I (convention model, yellow line) and Model II (proposed model, red line). Blue shows the inundation area at the start of the evacuation. The x- and y-axes indicate the axis in the Japan Plane Rectangular Coordinate System XII.

The number of successful evacuees at each evacuation start time is shown in Figure 7. The black line indicates the number of evacuees starting from nodes (i.e., the total number of people minus the number of people assigned to nodes already in the flooded area), the gray line indicates the number of successful evacuees for Model I, and the blue line indicates those for Model II. The number of successful evacuees in Model II is larger than that in Model I for all conditions. In particular, at time 60 min in Case (1), the number of successful evacuations for Model II is 2.16 times higher than that for Model I. Figure 8 shows the successful evacuation of the two models at the evacuation start time of 60 min for Case (1), in which Model II's improvement rate was the largest. Yellow points indicate successful evacuation, and purple points indicate failed evacuation. In Model I, the people in the direction of the extended flooded area cannot evacuate successfully. In Model II, however, most of the people can evacuate, except for those very close to the flooded area. This suggests that the proposed model has a higher success rate in case many evacuees cross areas of the extended floodplain to reach the shelter. Note that the number of evacuees starting decreases as the evacuation start time increases (black line in Figure 7). This is because the number of evacuees whose starting point is already caught in the flood area increases as the start of evacuation is delayed.

Figure 9 shows how the evacuation route changes when the function parameter C_d is changed in Model II (see Equation (1)). Figure 9a shows the result of Model I, and b–d are the results of different values of C_d. The red line indicates the searched evacuation route, and the yellow point indicates the location of the evacuation shelter. As C_d increases, a more diverted route is selected. By changing C_d, the degree of bypassing the flooded area can be determined. Figure 10a,b show the relationship between C_d and the cumulative number of successful evacuees for Case (1) and Case (3), respectively. In Case (1), the cumulative number of evacuees peaks when C_d = 1.0. This is because when C_d is smaller than 1, more evacuees choose routes closer to the flooded area and get caught in the flooded area. On the other hand, when C_d is larger than 1, more evacuees choose routes that essentially avoid the flooded area and thus, can be lengthier, consequently taking longer to evacuate. As a result, the flooded area becomes widespread during the evacuation, the number of available routes decreases, and the evacuation is more likely to fail. In Case (3), as C_d increases, the cumulative number of successful evacuees increases. This is because the pace of expansion of the flooded area is insignificant due to the storage-type flooding (i.e., a

flood type where levee breaches occur downstream of areas surrounded by levees), so even if evacuees choose routes that essentially avoid the flooded area, they will not get caught in the flooded area during the evacuation.

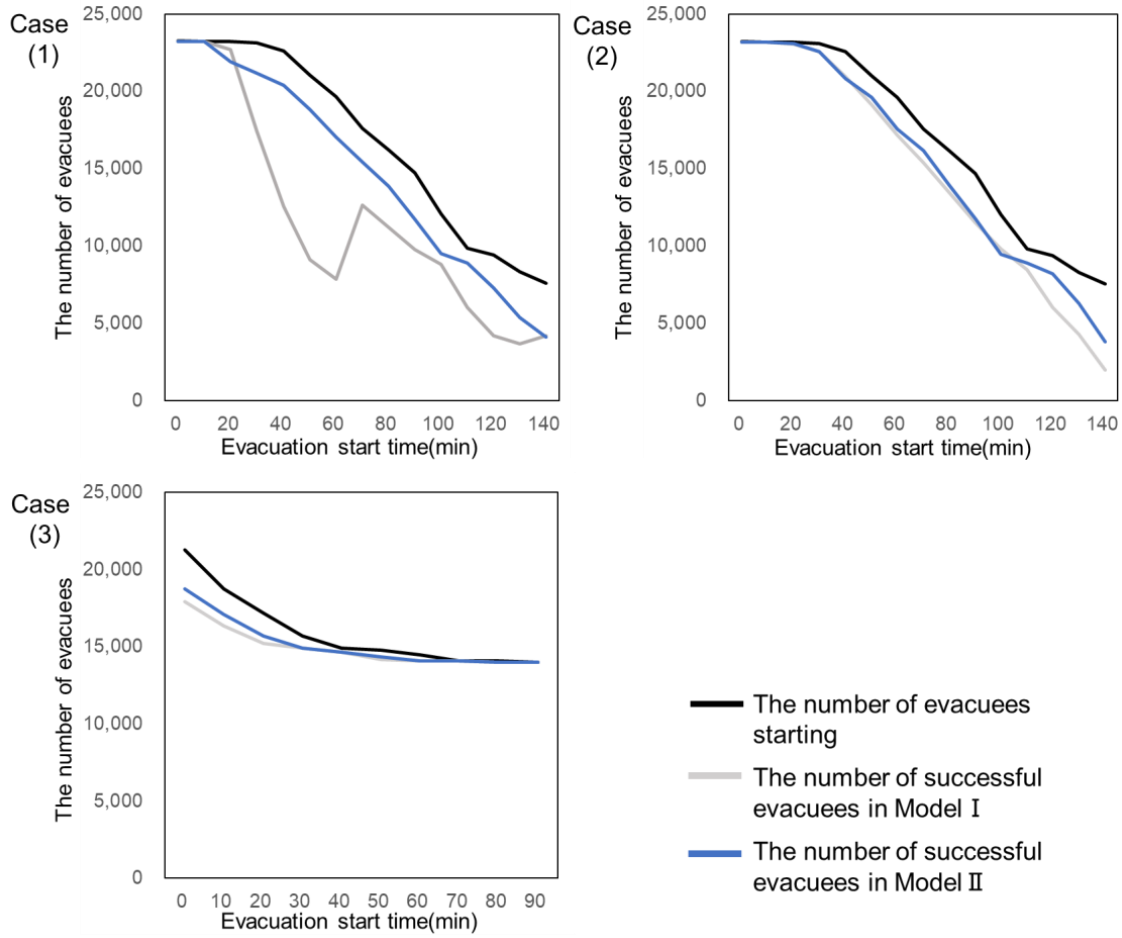

Figure 7. The number of successful evacuees at each evacuation start time. The black line indicates the number of evacuees starting from nodes (i.e., the total number of people minus the number of people assigned to nodes already in the flooded area); the gray line indicates the number of successful evacuees for Model I, and the blue line indicates those for Model II.

Although not included in this paper, we conducted similar simulations under multiple conditions by changing the location of the levee break and the shelter location. We found that the cumulative number of evacuees peaked at a C_d of approximately 1.0, regardless of the location of the levee breach or the shelter location. The results and analysis presented in this study show that the proposed model can be implemented to assess the safest evacuation routes in times of flooding. However, the analysis is still limited to the walking speed used in this study. That is, even if the inundation speed is slow, if the walking speed is slow, the number of successful evacuees may decrease as the C_d increases, as shown in Figure 10a. Conversely, even if the inundation speed is fast, if the evacuation speed is increased by using a car or other means, the number of successful evacuees may remain constant above a certain C_d, as shown in Figure 10b. In this study, the walking speed is set to be 4 km/h (i.e., the walking speed of a typical adult male), but this speed may vary depending on the age of the evacuee, the visibility conditions, the condition of the road e.g., [9–11], etc. Additionally, since evacuation by car during a flood has risks such as engine failure and inability to move due to rising water levels, this study assumes evacuation on foot. However, in reality, some people evacuate by car. That is, C_d should be modified according to gender, age, disability, way and time of evacuation, etc. Furthermore, a great deal of successful evacuation in times

of disaster depends upon the way the inhabitants at risk react to the situation. Hence, it is necessary to prepare and train the locals at risk to efficiently use the available evacuation systems/software and also establish a new attitude toward early disaster warnings and practicing early and timely evacuation.

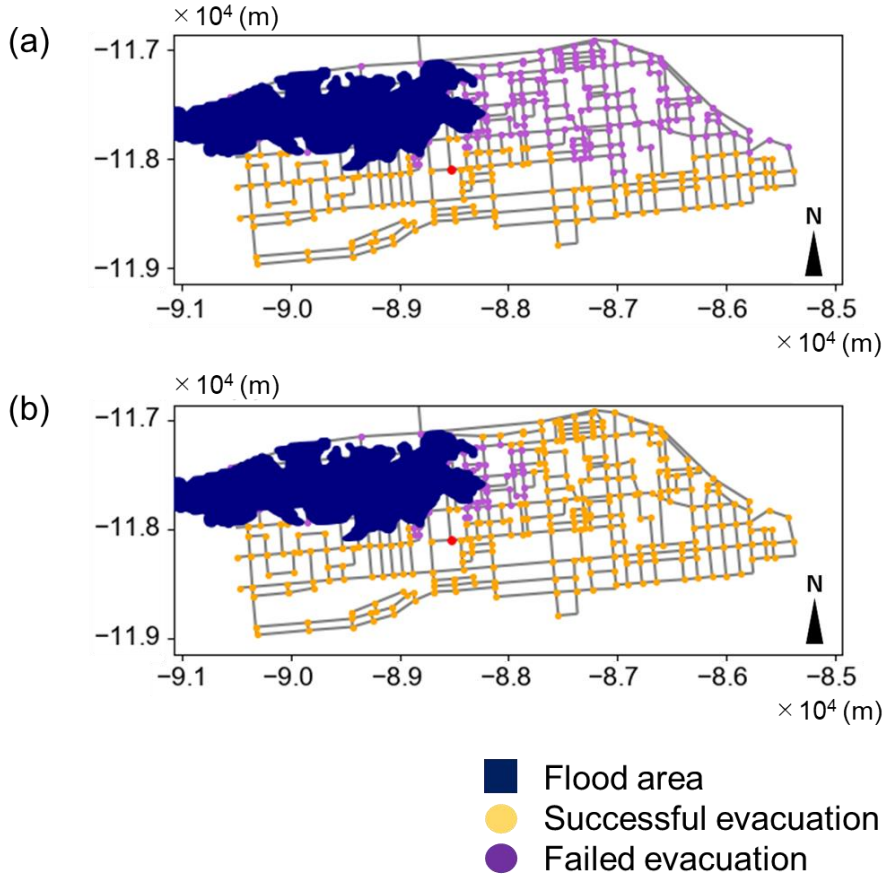

Figure 8. The evacuation conditions of the two models at the start time of evacuation t = 60 (min) in Case (1), (**a**) Model I, (**b**) Model II. Yellow points indicate successful evacuation, and purple points indicate failed evacuation. The x- and y-axes indicate the axis in the Japan Plane Rectangular Coordinate System XII.

While we consider only impassable roads due to inundation, bridges may become impassable during flooding owing to a variety of factors, such as damage to bridge piers caused by bed degradation, e.g., [25,26], the collapse of bridge abutments due to bank erosion, e.g., [24,27], lifting of bridge decks by water surface waves, e.g., [28–30]. The road data in this study does not include bridges over large rivers; however, it includes bridges over smaller rivers. It would be better if the model incorporated an indicator of bridge safety when a route across such bridges is chosen. Furthermore, if evacuation is difficult due to the damaged bridges, it may be crucial to evacuate to a higher floor of a building instead of evacuating to a shelter.

Since we mainly focus on developing a routing system in this study, we used flood simulations that we had run under simplified conditions. However, the technology for real-time flood mapping is growing every day [14–18]. The coupling of our model with real-time flood mapping could lead to the development of a real-time evacuation model that responds to the progression of flooding and provides safer evacuation routes that effectively avoid flooded areas. However, the role of Internet of Things (IoT) technology is important because real-time evacuation searches must provide evacuation routes based on the location of evacuees. Research on evacuation information related to IoT technology

has also progressed in recent years [15], and the integration with our system is an exciting future challenge.

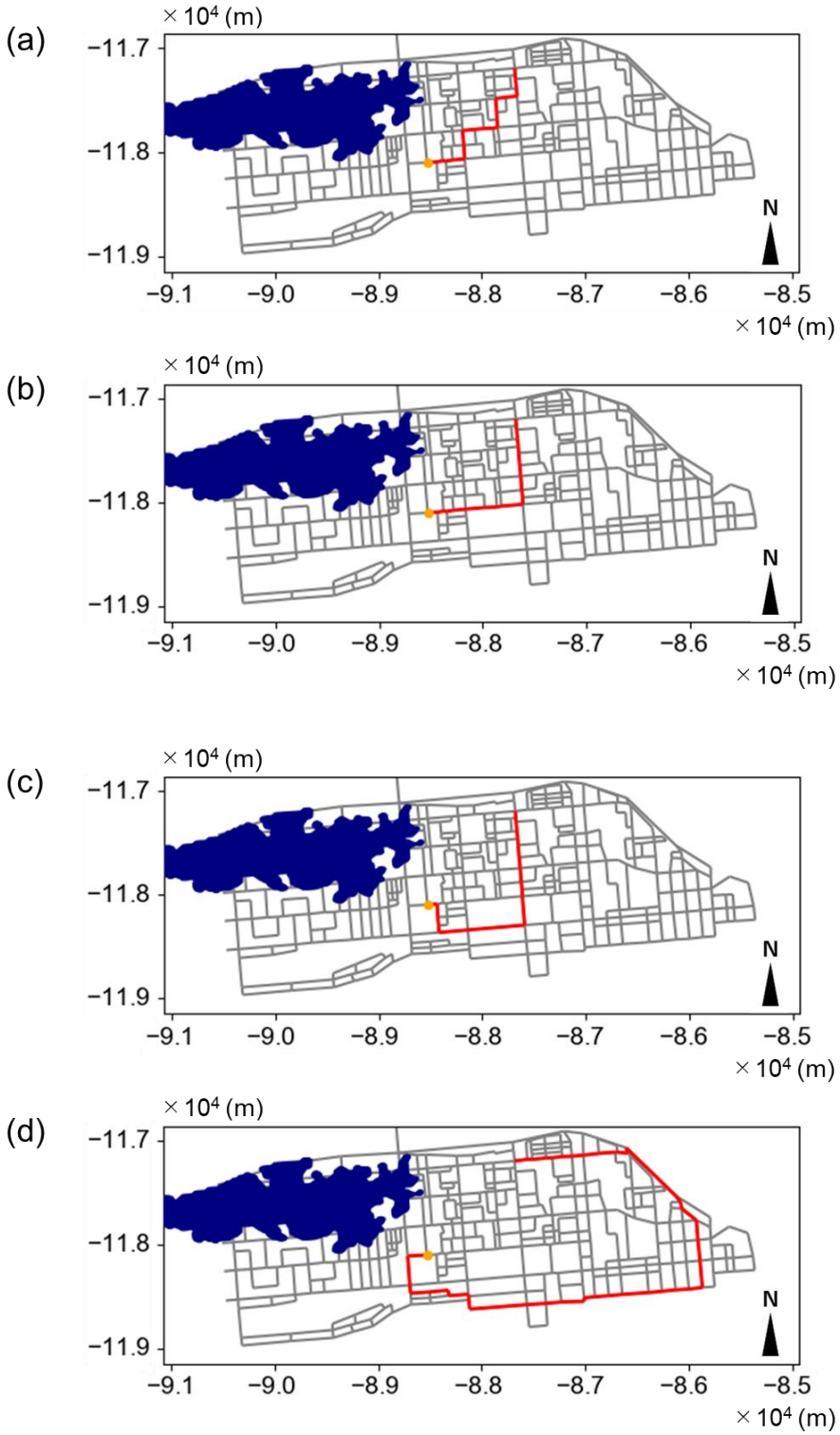

Figure 9. Evacuation route changes by model. (**a**) Model I; (**b**) C_d = 1 in Model II; (**c**) C_d = 5 in Model II; (**d**) C_d = 10 in Model II.

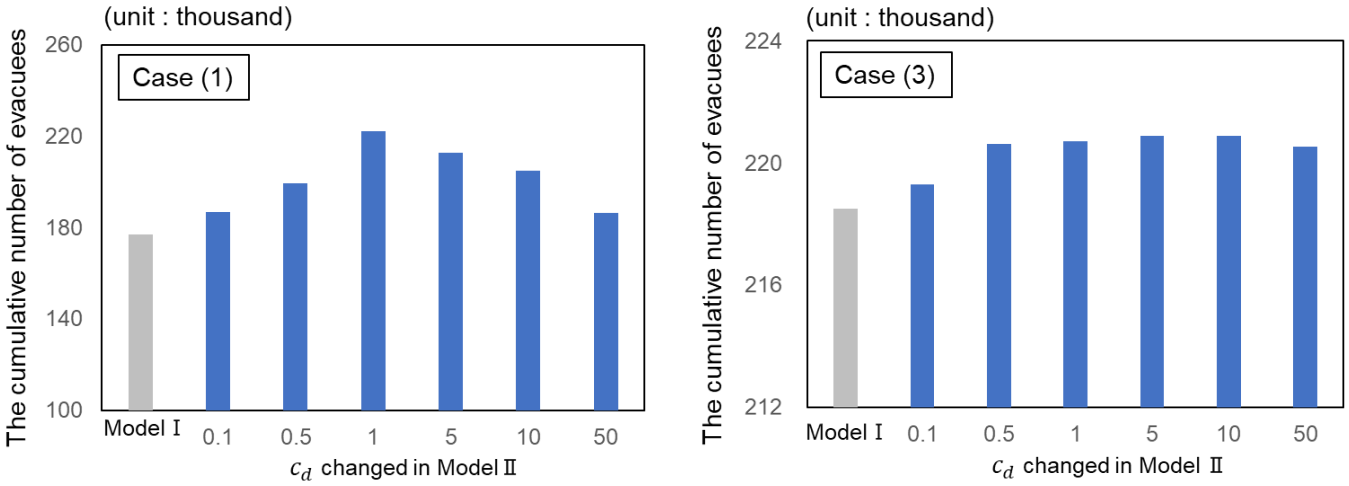

Figure 10. The cumulative number of successful evacuees when the model parameter C_d is changed. (**a**) Case (1); (**b**) Case (3).

4. Conclusions

In this study, we proposed a new evacuation route search system that takes into account the expansion speed of the flooded area. The analysis shows that our system can present safer evacuation routes using a simple function that uses the ratio of the distance that the flooded area has expanded over the previous 10-min period to the distance between the flooded area and the road. We performed three hypothetical flood simulations for Obihiro City, Japan, and compared our model with a conventional model that does not include the function. The number of successful evacuees in our model shows a maximum of 2.16 times increase against the conventional model. The model parameter that determines the degree of the detour of the evacuation route was generally constant at 1, regardless of the location of the breach or shelter in our study site.

Author Contributions: T.I. and Y.H. conceived the idea of the study; K.O. developed the system and performed the simulations; T.I., J.M. and Y.H. contributed to the interpretation of the results; T.I. supervised the conduct of this study; K.O. and J.M. drafted the manuscript with review, revision, and input from all authors. All authors have read and agreed to the published version of the manuscript.

Funding: This work was supported by Cross-ministerial Strategic Innovation Promotion Program (SIP) and JSPS KAKENHI Grant Number 22H01602. Participation in Jagriti Mishra was made possible by Ramanujan Fellowship no. RJF/2021/000168.

Institutional Review Board Statement: Not applicable.

Informed Consent Statement: Not applicable.

Data Availability Statement: The data are available from the corresponding author upon reasonable request.

Conflicts of Interest: The authors declare no conflict of Interest.

References

1. CRED. *2021 Disasters in Numbers*; CRED: Brussels, Belgium, 2021; Available online: https://cred.be/sites/default/files/2021_EMDAT_report.pdf (accessed on 5 December 2022).
2. River Data Book. 2022. Available online: https://www.mlit.go.jp/river/toukei_chousa/kasen_db/ (accessed on 5 December 2022). (In Japanese)
3. Chiu, Y.; Mirchandani, P.B. Online behavior-robust feedback information routing strategy for mass evacuation. *IEEE Trans. Intell. Transp. Syst.* **2008**, *9*, 264–274. [CrossRef]
4. Xie, C.; Lin, D.; Waller, S. A dynamic evacuation network optimization problem with lane reversal and crossing elimination strategies. *Transp. Res. Part E Logist. Transp. Rev.* **2010**, *46*, 295–316. [CrossRef]

5. Robinson, R.M.; Khattak, A. Route change decision Making by hurricane evacuees facing congestion. *Transp. Res. Rec.* **2010**, *2196*, 168–175. [CrossRef]
6. Lim, H.R.; Lim, M.B.B.; Piantanakulchai, M. A Review of Recent Studies on Flood Evacuation Planning. *J. East. Asia Soc. Transp. Stud.* **2013**, *10*, 147–162.
7. Chelariu, O.-E.; Iaţu, C.; Minea, I. A GIS-Based Model for Flood Shelter Locations and Pedestrian Evacuation Scenarios in a Rural Mountain Catchment in Romania. *Water* **2022**, *14*, 3074. [CrossRef]
8. Esposito Amideo, A.; Scaparra, M.P.; Kotiadis, K. Optimising shelter location and evacuation routing operations: The critical issues. *Eur. J. Oper. Res.* **2019**, *279*, 279–295. [CrossRef]
9. Musolino, G.; Ahmadian, R.; Xiia, J.; Falconer, R.A. Mapping the danger to life in flash flood events adopting a mechanics based methodology and planning evacuation routes. *J. Flood Risk Manag.* **2020**, *13*, e12627. [CrossRef]
10. Jonkman, S.N.; Penning-Rowsell, E. Human instability in flood flows. *JAWRA J. Am. Water Resour. Assoc.* **2008**, *44*, 1208–1218. [CrossRef]
11. Lee, H.K.; Hong, W.H.; Lee, Y.H. Experimental study on the influence of water depth on the evacuation speed of elderly people in flood conditions. *Int. J. Disaster Risk Reduct.* **2019**, *29*, 101198. [CrossRef]
12. Dash, N.; Gladwin, H. Evacuation decision making and behavioral responses: Individual and Household. *Nat. Hazards Rev.* **2007**, *8*, 69–77. [CrossRef]
13. Kievik, M.; Gutteling, J. Yes, we can: Motivate Dutch citizens to engage in self-protective behavior with regard to flood risks. *Nat. Hazards* **2011**, *5*, 1475–1490. [CrossRef]
14. Ming, X.; Liang, Q.; Xia, X.; Li, D.; Fowler, H.J. Real-time flood forecasting based on a high-performance 2-D hydrodynamic model and numerical weather predictions. *Water Resour. Res.* **2020**, *56*, e2019WR025583. [CrossRef]
15. Van Ackere, S.; Verbeurgt, J.; De Sloover, L.; Gautama, S.; De Wulf, A.; De Maeyer, P. A Review of the Internet of Floods: Near Real-Time Detection of a Flood Event and Its Impact. *Water* **2019**, *11*, 2275. [CrossRef]
16. Notti, D.; Giordan, D.; Caló, F.; Pepe, A.; Zucca, F.; Galve, J.P. Potential and Limitations of Open Satellite Data for Flood Mapping. *Remote Sens.* **2018**, *10*, 1673. [CrossRef]
17. Sekine, M.; WU, Y.; Baba, W.; Ogata, K. Prediction of urban inundation and flooding of urban rivers caused by heavy rainfall and storm surge in Tokyo 23 wards. In Proceedings of the 22nd IAHR-APD Congress, Sapporo, Japan, 15–16 September 2020.
18. Sekine's Urban Inundation Prediction System (S-uiPS) Open to the Public in September 2022. Available online: https://kyodonewsprwire.jp/release/202209066029 (accessed on 5 December 2022). (In Japanese).
19. Inoue, T.; Nakatani, T.; Yabe, H. Route search with real-time flood prediction. *J. Jpn. Soc. Civ. Eng. Ser. B1 (Hydraul. Eng.)* **2018**, *74*, I_1291–I_1296. (In Japanese) [CrossRef] [PubMed]
20. Lee, Y.H.; Kim, H.I.; Han, K.Y.; Hong, W.H. Flood Evacuation Routes Based on Spatiotemporal Inundation Risk Assessment. *Water* **2020**, *12*, 2271. [CrossRef]
21. Krytska, Y.; Skarga-Bandurova, I.; Velykzhanin, A. IoT-based situation awareness support system for real-time emergency management. In Proceedings of the 9th IEEE International Conference on Intelligent Data Acquisition and Advanced Computing Systems: Technology and Applications (IDAACS), Bucharest, Romania, 21–23 September 2017; Volume 2, pp. 955–960.
22. Nishikawa, S.; Hori, T. Effect of obstacle information sharing among evacuees on flood evacuation. *J. Jpn. Soc. Civ. Eng.* **2019**, *75*, 1327–1332.
23. Nelson, J.M.; Shimizu, Y.; Abe, T.; Asahi, K.; Gamou, M.; Inoue, T.; Iwasaki, T.; Kakinuma, T.; Kawamura, S.; Kimura, I.; et al. The international river interface cooperative: Public domain flow and morphodynamics software for education and applications. *Adv. Water Resour.* **2016**, *93*, 62–74. [CrossRef]
24. Shimizu, Y.; Nelson, J.; Arnez, K.F.; Asahi, K.; Giri, S.; Inoue, T.; Iwasaki, T.; Jang, C.L.; Kang, T.; Kimura, I.; et al. Advances in computational morphodynamics using the International River Interface Cooperative (iRIC) software. *Earth Surf. Process. Land.* **2019**, *45*, 11–37. [CrossRef]
25. Inoue, T.; Mishra, J.; Kato, K.; Sumner, T.; Shimizu, Y. Supplied sediment tracking for bridge collapse with large-scale channel migration. *Water* **2020**, *12*, 1881. [CrossRef]
26. Pizarro, A.; Manfreda, S.; Tubaldi, E. The Science behind Scour at Bridge Foundations: A Review. *Water* **2020**, *12*, 374. [CrossRef]
27. Sumner, T.; Inoue, T.; Shimizu, Y. The influence of bed slope change on erosional morphology. *J. JSCE* **2019**, *7*, 15–21. [CrossRef] [PubMed]
28. Johnson, P.A.; Whittington, R.M. Vulnerability-Based Risk Assessment for Stream Instability at Bridges. *J. Hydraul. Eng.* **2011**, *137*, 1248–1256. [CrossRef]
29. Huang, W.; Xiao, H. Numerical modeling of dynamic wave force acting on Escambia bay bridge deck during Hurricane Ivan. *J. Waterw. Port Coast. Ocean. Eng.* **2009**, *135*, 164e175. [CrossRef]
30. Inoue, T.; Watanabe, Y.; Iwasaki, T.; Otsuka, J. Three-dimensional antidunes coexisting with alternate bars. *Earth Surf. Process. Landf.* **2020**, *45*, 2897–2911. [CrossRef]